BATCH REMOVAL OF MANGANESE FROM ACID MINE DRAINAGE USING BONE CHAR

D. C. Sicupira[1], T. Tolentino Silva[1], V. A. Leão[2] and M. B. Mansur[1*]

[1]Departamento de Engenharia Metalúrgica e de Materiais, Universidade Federal de Minas Gerais,
Phone: + (55) (31) 3409-1811, Fax: + (55) (31) 3409-1716, Av. Antônio Carlos 6627,
Campus Pampulha, CEP: 31270-901, Belo Horizonte - MG, Brazil.
E-mail: marcelo.mansur@demet.ufmg.br
[2]Departamento de Engenharia Metalúrgica e de Materiais, Phone: + (55) (31) 3559-1102,
Fax: + (55) (31) 3559-156, Universidade Federal de Ouro Preto, Campus Universitário,
Morro do Cruzeiro, CEP: 35400-000, Ouro Preto, Belo Horizonte - MG, Brazil.
E-mail: versiane@demet.em.ufop.br

Abstract - The present study investigated batch kinetics and the batch equilibrium of manganese removal from acid mine drainage (AMD) using bone char as an adsorbent. Equilibrium tests revealed that the Langmuir-based maximum manganese uptake capacity was 22 mg g^{-1} for AMD effluents and 20 mg g^{-1} for laboratory solutions at a pH ranging from 5.5 to 5.7. The pseudo-second order model best described the manganese kinetics within bone char. Manganese removal was mainly influenced by the operating variables of the solid/liquid ratio and the pH of the aqueous phase. In fact, metal uptake was favored at nearly neutral pH values. The effect of particle size and temperature proved to be insignificant for the investigated operating range. This work also evaluated the mechanism for manganese removal using bone char. Results showed that intraparticle diffusion is the main rate-limiting step; however, additional contributions from boundary layer diffusion may well affect this removal when particles of smaller sizes are used. The final concentration of fluoride and other metals present in the AMD effluent was in agreement with the concentration limit set forth by Brazilian legislation. The present study demonstrated that bone char is a suitable material to be used for the removal of manganese from AMD effluents.
Keywords: Manganese; Bone char; Acid mine drainage; Adsorption.

INTRODUCTION

The generation of acid mine drainage (AMD) is one of the most serious environmental problems faced by the mining industry nowadays. AMD occurs when pyrite and/or other sulfide minerals are oxidized due to their exposure to oxygen and water, thus producing sulfuric acid that can dissolve metal species, resulting in the contamination of the environment (Nascimento, 1998). The main sources of AMD are open or underground pit mines, waste rock piles, tailings storage, and ore stockpiles. The rise in the concentration of metal ions in the percolating waters due to AMD is an important source of contamination of water courses, particularly when ions can be spread to the food chain. Aimed at minimizing the severity of such impacts, environmental protection laws require appropriate plans for mine closures in an attempt to increase the life cycle of closed mines, including steps of decommissioning and the recovery of degraded areas (Ladeira and Gonçalves, 2008).

In Brazil, AMD has been identified in coalfields in the southern regions of the country. Particularly in the state of Minas Gerais, the AMD generated in the region of Poços de Caldas contains radionuclides (uranium, thorium, radium, among others), as well as species like manganese, zinc, fluoride, and iron at concentration levels that exceed those authorized by Brazilian legislation for direct discharge (CONAMA, 2005; Ladeira and Gonçalves, 2008). The current

*To whom correspondence should be addressed

treatment of such acid waters consists of metals precipitation with lime followed by pH correction. Most metal species are precipitated, but the removal of manganese ions from AMD is notoriously difficult due to their complex chemistry in aqueous systems (Bamforth *et al.,* 2006; Robinson-Lora and Brennan, 2010). In fact, for full precipitation of manganese as $Mn(OH)_2$, the pH must be raised to approximately 11, which involves a significant consumption of lime (Ladeira and Gonçalves, 2008). After manganese removal, the pH must then be neutralized before discharge. Therefore, such treatment is costly and generates large volumes of sludge. As a result, new technologies to treat AMD effluents containing manganese are of utmost importance.

The adsorption of metal species has been investigated using various alternative materials (Korn *et al., 2004*; Bosco *et al., 2005*; Soto *et al.*, 2005), but little attention has been given to manganese removal from AMD solutions. Adsorption has proven to be a particularly interesting technique in hydrometallurgical applications. It allows for the removal of ions from very dilute solutions and possesses the ability to process large volumes of solutions when other separating methods seem unfavorable.

Bone char has been successfully applied for the removal of various metal species, such as copper, zinc, cadmium, arsenic, and mercury, among others (Cheung *et al.*, 2000; Choy *et al.*, 2004; Chen *et al.*, 2008; Hassan *et al.*, 2008; Pan *et al.*, 2009); however, to date, the specific use of bone char to remove manganese from AMD effluents has yet to be experimented. As bone char consists basically of hydroxyapatite $(Ca_{10}(PO_4)_6(OH)_2)$ and calcite $(CaCO_3)$, its use could not only remove metals species, but also raise the pH of the effluent due to the dissolution of the calcite, thus contributing to a reduction in the lime consumption used in the current treatment of AMD solutions containing manganese.

Therefore, the present work evaluated the feasibility of using bone char in the treatment of AMD effluents containing manganese. For this attempt, batch equilibrium and kinetics tests were performed using both AMD effluents and laboratory solutions containing manganese at typical concentrations for comparative analysis.

EXPERIMENTAL

Reagents and Instrumentation

The present study used AMD effluents generated in a closed uranium mine located in the state of Minas Gerais, Brazil, and bone char (Bone Char do Brasil Ltda). A laboratory solution containing 100 mg L^{-1} of manganese was also prepared using chemicals of analytical reagent grade dissolved in distilled water.

A mechanical shaker (Nova Ética 109) was used to agitate the sample solutions with bone char. An atomic emission spectrometer with inductively coupled plasma (ICP-AES Perkin Elmer OPTIMA 7300DV) was used to assess the concentration of manganese in the aqueous solutions. Sulfate and fluoride analyses were performed using a DX500 Dionex ion chromatograph. The pH of the aqueous solutions was measured using a pH meter (Quimis). Scanning electron microscopy (SEM, Jeol JSM 5410) with X-ray energy dispersive spectrometry (EDS, Noran Voyager 3.4.1) was employed to analyze the surface morphology and to obtain the elemental composition of the bone char, which was also analyzed by X-ray diffraction (XRD, PANalytical X'Pert APD diffractometer) and Fourier transform infra-red (FTIR, Perkin Elmer Paragon 1000 spectrometer). In addition, surface area, total pore volume, and average pore diameter were assessed by measuring multipoint N_2 isotherms in a BET Quantachrome model Autosorb 1C.

Manganese Removal Studies

Batch Sorption Kinetics

Kinetics tests were carried out using 400 mL of laboratory solution or mining effluent at room temperature. The solutions were mixed with 2 g of bone char (solid/liquid ratio = 2/400 g mL^{-1}), and the mixture was magnetically stirred for 48 hours at a rotation speed of 150 min^{-1}. The pH remained constant (around neutral) due to the buffer effect from the calcite dissolution.

Samples of the aqueous solutions (1 mL) were collected at fixed contact times, diluted, filtered, and acidified using HNO_3 before being analyzed by ICP-AES. The influence of the solid/liquid ratio on the sorption kinetics of manganese was studied using different amounts of bone char, i.e., 1, 2, and 3 g (solid/liquid ratio 1/400, 2/400, and 3/400 g mL^{-1}, respectively). Sorption kinetics studies were also carried out using bone char samples of different particle sizes (417-833 μm, 104-147 μm, and <53 μm).

Batch Sorption Isotherms

A series of tests was performed in the concentration range from 10 to 100 mg L^{-1} using the AMD effluent and laboratory solutions. Aliquots of 100 mL of each solution were placed in Erlenmeyer

flasks. The pH of the effluent was first adjusted to 5.0 or 6.5, using a $Ca(OH)_2$ solution (30%) in order to precipitate other metals, and then filtered. The laboratory solutions received no pH adjustment (initial pH = 5.7). In each flask, 250 mg of bone char was added, and the suspension was shaken at 150 min^{-1}, at a room temperature of 25 ºC, using a mechanical shaker for 48 hours. The effects of the following operating variables were investigated: initial pH of the effluent (5.0 and 6.5) and temperature (10 ºC, 25 ºC, and 40 ºC). After agitation, the suspension was filtered, and the filtrate was analyzed by ICP-AES to assess the metal concentration.

RESULTS AND DISCUSSION

Characterization Analysis

Characterization of the Bone Char

The bone char has a real density of 2.9 g cm^{-3}. Pore distribution measurements revealed that bone char samples with particle size <53 μm and 417-833 μm

contain 94.7% and 86.5% of macropores (pore sizes greater than 50 nm, according to the IUPAC classification given by Rouquerol *et al.,* 1994), respectively. As the presence of micropores (pore size below 2 nm) was insignificant, mesopores (pore sizes between 2 and 50 nm) represent 5.3% and 13.5%, respectively. As a consequence of its porous nature (total pore volume 0.275 cm^3 g^{-1}), bone char shows a surface area of 93 m^2 g^{-1}.

As regards the composition of bone char, XRD analysis revealed that the main phases of bone char are hydroxyapatite $(Ca_{10}(PO_4)_6(OH)_2)$ and calcite $(CaCO_3)$. The presence of such species was corroborated by FTIR spectral analysis. The morphology and chemical composition of bone char, assessed by SEM-EDS before its contact with the AMD effluent (Figures 1(a) and 1(b), respectively), revealed a significant presence of calcium and phosphorus. After the adsorption process (Figures 1(c) and 1(d), a decrease in the relative Ca/P ratio was observed due to the dissolution of calcite. Also verified was the presence of manganese and others species (F, S, La, Ce), thus suggesting that such elements are present on the surface of the loaded bone char, possibly due to some adsorptive and/or precipitating process.
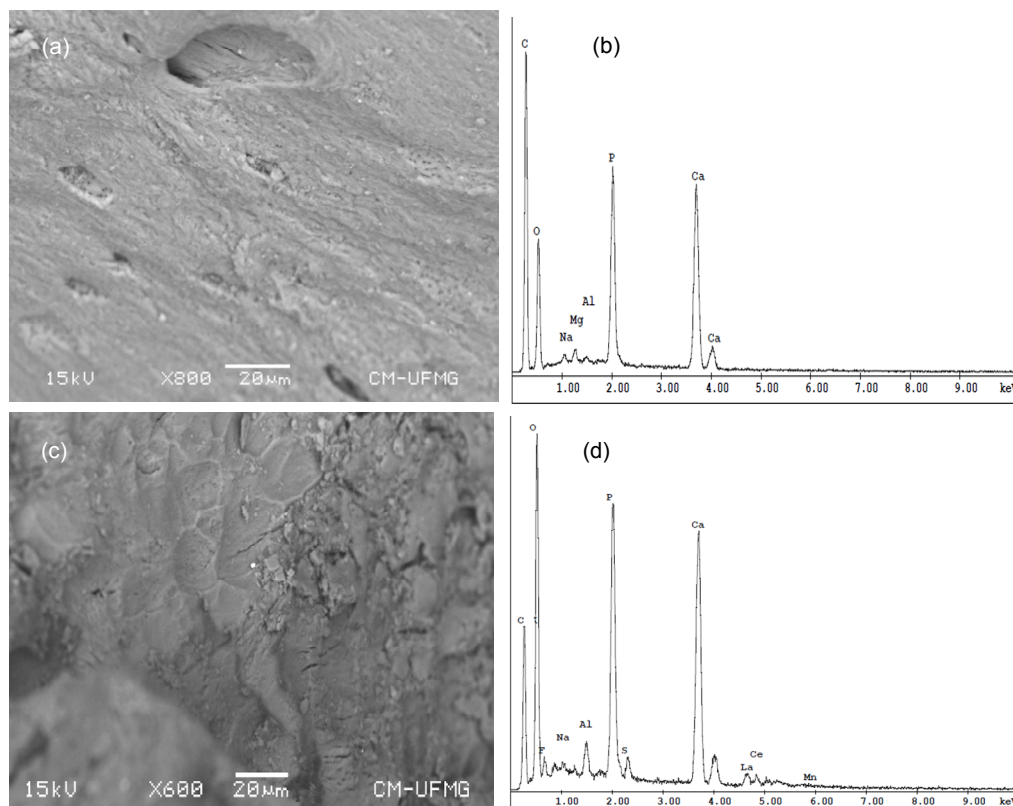

Figure 1: Morphology and chemical composition of bone char by SEM-EDS: (a), (b) bone char as received and (c), (d) bone char after contact with AMD effluent.

Characterization of the AMD Effluent

The composition of the AMD effluent before and after precipitation with $Ca(OH)_2$ is shown in Table 1, which includes the concentration limits of species authorized by Brazilian laws regarding effluent discharge (CONAMA, 2005). It could be verified that the manganese concentration in the AMD far exceeded the maximum levels permitted by law. The same process occurs with zinc and acidity. Thus, the treatment of effluents is mandatory. By contrast, the concentration of iron proved to be acceptable for discharge. After precipitation with $Ca(OH)_2$, it could be observed that the manganese concentration was still not in agreement with Brazilian regulations. However, the concentration of the other elements present in the AMD effluent, except for fluoride, were within acceptable limits.

Batch Sorption Kinetics

Experimental kinetic data were linearized using the pseudo-second order kinetic equation, and a satisfactory fit was obtained ($R^2 \geq 0.98$ for all cases), according to the following equation:

$$\frac{t}{q_t} = \frac{1}{k_2 q_e^2} + \frac{t}{q_e} \tag{1}$$

in which q_t (mg g^{-1}) is the amount of manganese adsorbed in the bone char at time t, q_e (mg g^{-1}) is its value at equilibrium, and k_2 (g mg^{-1} min^{-1}) is a constant of the pseudo-second-order adsorption model.

The equilibrium adsorption capacity q_e and the second-order constants k_2 were determined experimentally from the slope and the intercept of the plot of t/q_t *versus time*, respectively. In general, the pseudo-second order model is used to describe chemisorption mechanisms (Ho, 2006).

The effect of the solid/liquid ratio on the adsorption kinetics of manganese is shown in Figures 2(a) and 2(b) for the laboratory solution containing only manganese and for the AMD effluent, respectively. As expected, a higher percentage of manganese removal was obtained with the increase in the solid/liquid ratio for both solutions. In addition, a longer time was required to load the adsorbent with the increase in the solid/liquid ratio. The effect of competing species present in the AMD effluent for the adsorbent is shown in Figure 2(b), resulting in a significant reduction in the manganese removal efficiency when compared to the laboratory solution. Such a result highlights the necessity to raise the pH of the effluent before treatment in order to increase the loading of the bone char for the specific removal of manganese. The effect of competing species was verified in the calculated q_e values (for the laboratory solution, q_e was 19, 17, and 13 mg g^{-1}, whereas for the AMD effluent, q_e was 14, 10, and 7 mg g^{-1}, at a changing solid/liquid ratio of 1/400, 2/400, and 3/400 g mL^{-1}, respectively). In fact, lower values were obtained when the AMD effluent was used, as well as when the solid/liquid ratio for both solutions was increased, as expected. The final pH values of the solutions were kept constant in the range of 7.2 to 7.4 due to the buffering effect from the calcite dissolution.

Table 1: Chemical characterization of the AMD effluent and concentration limits according to Brazilian law (CONAMA, 2005).

Parameters*	Concentration (mg L^{-1})	Concentration after precipitation (mg L^{-1})	CONAMA 357 (mg L^{-1})
U	6.8	<0.3	-
Mn	107.5	89.5	1.0
Ca	104.9	428	-
Mg	7.6	7.4	-
Al	164.2	28.5	-
Zn	17.7	4.0	5.0
Fe	<0.01	<0.01	15.0
F^-	99.0	38.0	10.0
SO_4^{2-}	1349	1335	-
pH	2.97	5.64	6 to 9

* All parameters are expressed in mg L^{-1}, except pH.
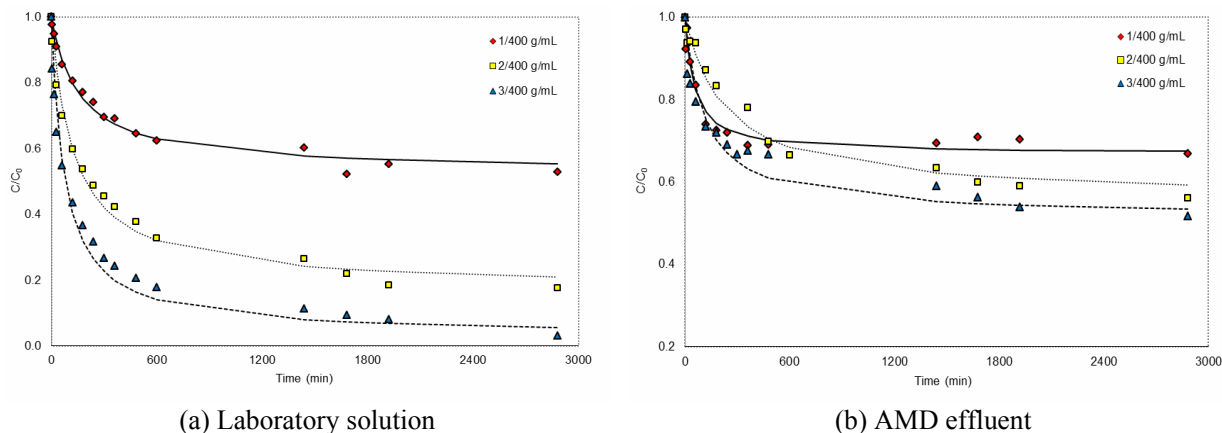- Permissible level not defined by Brazilian law.

(a) Laboratory solution   (b) AMD effluent

Figure 2: Effect of solid/liquid ratio on the kinetics of manganese removal with bone char (25 °C, 150 min^{-1}, 417-833 μm, continuous curves are pseudo-second order model): (a) Laboratory solution ($C_0 = 100$ mg L^{-1}, pH$_i$ = 5.76) and (b) AMD effluent (pH$_i$ = 5.64).

Regarding the effect of particle size, the results obtained for the laboratory solution (Figure 3(a)) and AMD effluent (Figure 3(b)) revealed that the different particle size ranges analyzed in this study have little effect on the manganese adsorption at longer times; however, the loading kinetics were affected. As expected, the higher k_2 values for smaller particle size indicated that the time needed to reach equilibrium is shorter for the smaller particle size (for the laboratory solution, k_2 was 0.51, 3.80, and 5.60 mg g^{-1} min^{-1}, whereas for the AMD effluent, k_2 was 0.44, 1.60, and 2.00 mg g^{-1} min^{-1}, for particle sizes of 417-833, 104-147, and <53 μm, respectively). The values of q_e obtained for different particle sizes are relatively close (for the laboratory solution, q_e was 17, 18, and 18 mg g^{-1}, whereas for the AMD effluent, q_e was 10, 10, and 13 mg g^{-1}, for

particle sizes of 417-833, 104-147, and <53 μm, respectively), but the effect of competing species present in the AMD effluent for the adsorbent shown in Figure 3(b) results in a significant reduction in manganese removal. The final pH of the solution was kept constant in the range of 7.2 to 7.5.

Ozawa *et al.* (2003) used fish bone-hydroxyapatite for manganese removal from laboratory solutions. The initial concentration of Mn(II) was 16 mg L^{-1}, and 0.3 g of the bone powder was added to each 2 L of aqueous solution. After the mixture of powder and solution had been stirred for 2 hours and held for 6 days without stirring, the maximum adsorption capacity reached 17 mg g^{-1}. This value of maximum loading is quite close to the values obtained in the present kinetic study for manganese removal using bone char.
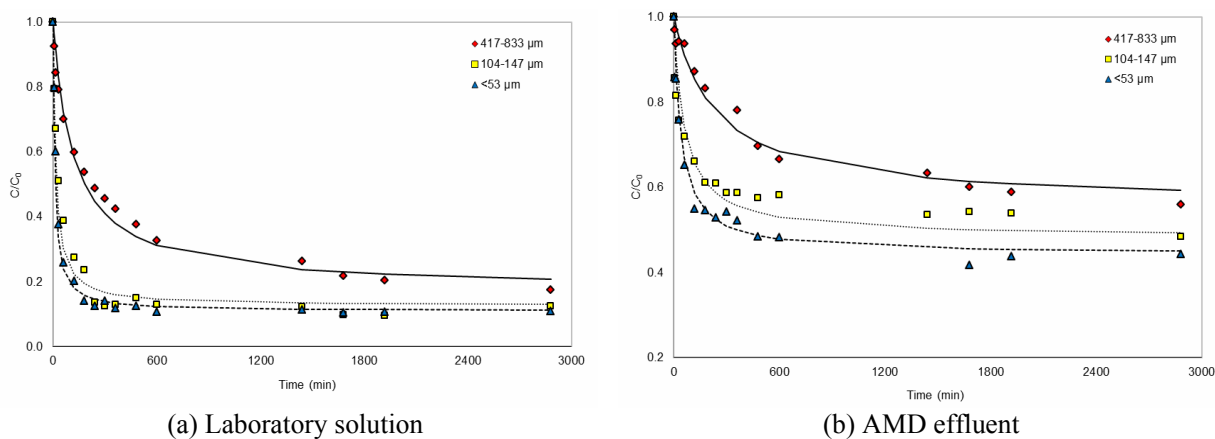

(a) Laboratory solution   (b) AMD effluent

Figure 3: Effect of particle size on the kinetics of manganese removal with bone char (25 °C, 150 min^{-1}, 2/400 g mL^{-1}, continuous curves are pseudo-second order model): (a) Laboratory solution ($C_0 = 100$ mg L^{-1}, pH$_i$ = 5.76) and (b) AMD effluent (pH$_i$ = 5.64).

Batch Sorption Isotherms

The Langmuir adsorption isotherm proved to be appropriate enough to fit the experimental data of manganese adsorption onto the bone char within the investigated conditions ($R^2 \geq 0.98$ for all cases). The saturation monolayer is given by the following expression in linear form:

$$\frac{1}{q_e} = \frac{1}{q_m} + \frac{1}{bq_m C_e} \qquad (2)$$

in which q_e (mg g^{-1}) is the adsorption capacity by weight at equilibrium, q_m (mg g^{-1}) is the theoretical maximum adsorption capacity by weight, b (L mg^{-1}) represents the Langmuir constant, and C_e (mg L^{-1}) is the concentration of adsorbate in the aqueous phase at equilibrium (Annadurai *et al.*, 2008).

The effect of the initial pH of the AMD effluent on the removal of manganese is shown in Figure 4. As indicated by the equilibrium data, the removal of manganese is more effective when the initial pH of the effluent was raised to 6.5 due to the precipitation of certain metals present in the liquor. Preliminary tests have pointed out that pH ranging from 7.0 to 7.5 would be ideal for the adsorption of manganese. In fact, when the initial pH of the effluent was set to 5.0, the final pH was 6.0, and when the initial pH was 6.5, its final value was 7.4, thus attending to Brazilian norms in both situations (see Table 1). The rise in pH when the AMD effluent comes into contact with the bone char is attributed to the dissolution of calcite present in the adsorbent. Therefore, for the solid/liquid ratio used in this experiment, initial pH = 6.5 results in a higher value of q_m for the manganese adsorption from the AMD

effluent ($q_m = 14$ mg g^{-1} and b = 0.43 L mol^{-1} at pH$_i$ = 5.0, whereas $q_m = 22$ mg g^{-1} and b = 0.47 L mol^{-1} at pH$_i$ = 6.5). For laboratory solutions, the effect of the initial pH was not studied, as adjustments were not necessary.
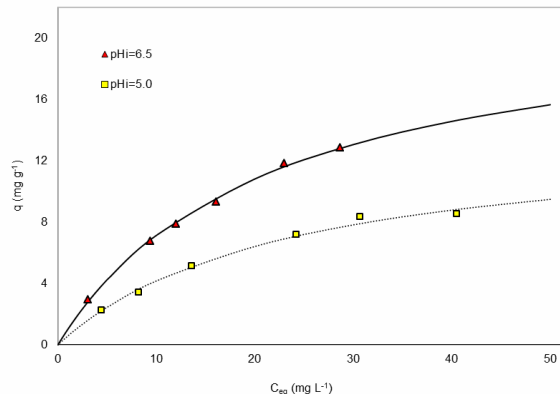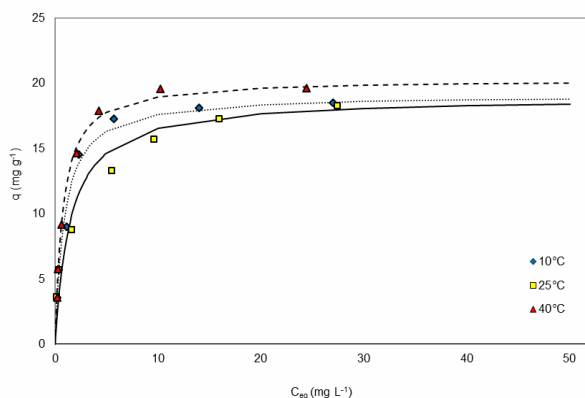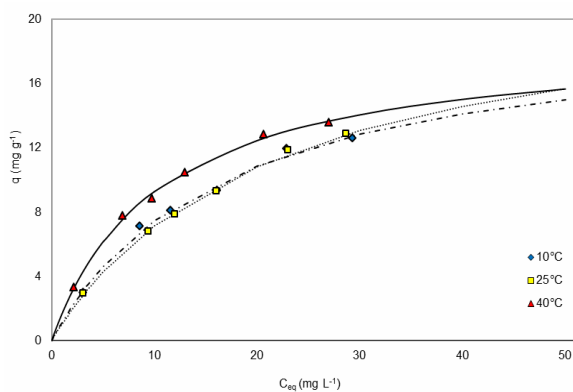

Figure 4: Effect of initial pH on the isotherm for manganese removal from AMD effluent with bone char (25 °C, 150 rpm, 53 μm, 0.25/100 g mL^{-1}, 48 hours; continuous lines are Langmuir model).

The effect of temperature on manganese removal from laboratory solutions and AMD effluents (Figure 5) revealed that such a parameter has little impact on the manganese adsorption within the investigated range (for the laboratory solution, q_m was 19, 19, and 20 mg g^{-1}, whereas for the AMD effluent, q_m was 20, 22, and 19 mg g^{-1}, at temperatures of 10 °C, 25 °C, and 40 °C, respectively). Therefore, it is expected that manganese removal with bone char will not be significantly affected by the seasonal temperature changes in the region where AMD is generated.

(a) Laboratory solution

(b) AMD effluent

Figure 5: Effect of temperature on the isotherm for manganese removal with bone char (150 rpm, <53 μm, 1/400 g mL^{-1}, 48 hours; continuous lines are Langmuir model): (a) Laboratory solution ($C_0 = 100$ mg L^{-1}, pH$_i$ = 5.76) and (b) AMD effluent (pH$_i$ = 5.64).

Finally, analysis of the liquor at 25 °C revealed that fluoride species were also removed by the bone char. In fact, fluoride concentrations in the AMD effluent meet Brazilian standards (CONAMA, 2005) and proved to be smaller than the detection limit of the technique used (<0.6 mg L^{-1}).

Mechanism of Manganese Removal with Bone Char

The removal of cations from aqueous solutions by hydroxyapatite may generally occur due to different sorption processes (adsorption, ion-exchange, surface complexation, co-precipitation, recrystalization) depending on the experimental conditions as well as on the nature of both sorbing cations and the hydroxyapatite itself. Smiciklas *et al.* (2000) reported that acidic as well as basic solutions in pH ranging from 4 to 10 can be buffered after reaction with the reactive surface sites of hydroxyapatite to the pH_{pzc} value in which the surface charge is zero.

According to Pan *et al.* (2009), the surface charge of hydroxyapatite is predominated by positively charged $\equiv CaOH_2^+$ and neutral $\equiv POH^0$ species in acid solutions; thus, the surface charge of hydroxyapatite in these pH conditions is positive. On the other hand, in alkaline solutions, neutral $\equiv CaOH^0$ and negatively charged $\equiv PO^-$ species may prevail on the hydroxyapatite surface, thus becoming negatively charged:

$$\equiv CaOH_2^+ \leftrightarrows \equiv CaOH^0 + H^+ \qquad (3)$$

$$\equiv PO^- + H^+ \leftrightarrows \equiv POH^0 \qquad (4)$$

The electrical characteristics of bone char were evaluated based on zeta potential measurements as defined by Rocha *et al.* (2012), the results of which showed that the surface of the bone char was predominantly negatively charged in pH values of above 5. This can increase the electrostatic attraction forces between the bone char surface and the cations in the solution, thus favoring the sorption of cations from aqueous solutions with pH > 5.

To investigate the release of calcium to the solution, the bone char was washed, as described by Ribeiro (2011), aimed at dissolving the calcite from the solid phase. The calcium released to the solution showed that an ion exchange mechanism was involved in the removal of manganese from AMD (a linear relationship is shown in Figure 6). According to O'Connor and Weatherley (1997), the hy-

droxyapatite from the bone char plays an important role in the adsorption of manganese, with adsorption occurring by ion exchange.
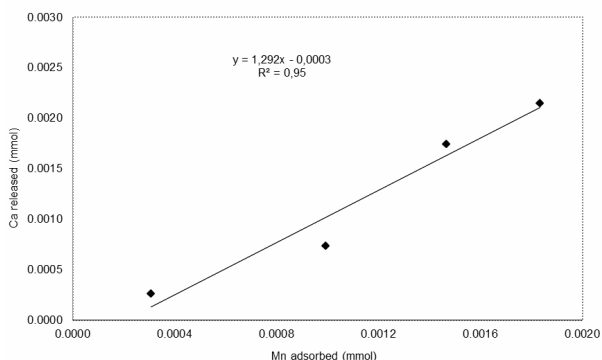

Figure 6: Relationship between release of calcium into solution and manganese adsorbed onto bone char (Laboratory solution, pH_i = 5.76, C_0 = 100 mg L^{-1}, 25 °C, 150 min^{-1}, 417–833 µm, 0.25/100 g mL^{-1}, 24 hours).

The effect of diffusion as the rate controlling mechanism in the manganese removal by bone char was evaluated according to the intraparticle diffusion model. It is well-known that intraparticle diffusion plays a significant role in many adsorption processes and that the most significant contribution for the kinetic-mass transfer process is most commonly due to the diffusion of adsorbate within the porous structure of the adsorbent. The intraparticle diffusion model for adsorption is given by the following equation (Weber and Morris, 1963):

$$q_t = k_p \sqrt{t} + C \qquad (5)$$

in which k_p is the intraparticle diffusion constant, which is evaluated as the slope of the curve q_t *versus* $t^{1/2}$, and C is the constant related to the boundary layer thickness. If the regression of q_t versus $t^{1/2}$ is linear and passes through the origin, then intraparticle diffusion is the sole rate-limiting step.

To evaluate the effect of intraparticle diffusion on the manganese adsorption process, q_t was plotted as a function of the square root of time, $t^{1/2}$, at different particle size fractions for the laboratory solution and AMD effluent (see Figure 7). The plot for intraparticle diffusion revealed a linear behavior passing near to the origin at the beginning of the manganese adsorption process (until 180 min for the particle size range of <53 and 104-147 µm, and until 600 min for the particle size range of 417-833 µm). This finding indicates that intraparticle diffusion is the main rate-

limiting step for manganese sorption systems, but not the sole rate-limiting step, given that the plot for intraparticle diffusion passes near its origin. The calculated k_p values revealed that the intraparticle diffusion effect becomes less significant when the particle size increases. Therefore, manganese removal becomes slower (for the laboratory solution, k_p was 0.53, 1.00, and 1.06 mg g^{-1} min$^{-0.5}$, whereas for the AMD effluent, k_p was 0.29, 0.44, and 0.66 mg g^{-1} min$^{-0.5}$, at particle sizes of 417-833, 104-147, and <53 μm, respectively). The C constant values indicate that the larger the intercept, the greater the boundary layer effect (Annadurai *et al.*, 2008). Therefore, based on the calculated results (for the laboratory solution, C was 1.41, 3.10, and 2.02 mg g^{-1}, whereas for the AMD effluent, C was 0.05, 2.21, and 1.95 mg g^{-1}, at particle sizes of 417-833, 104-147 and <53 μm, respectively), the effect of external resistance increased when smaller particle sizes were used.
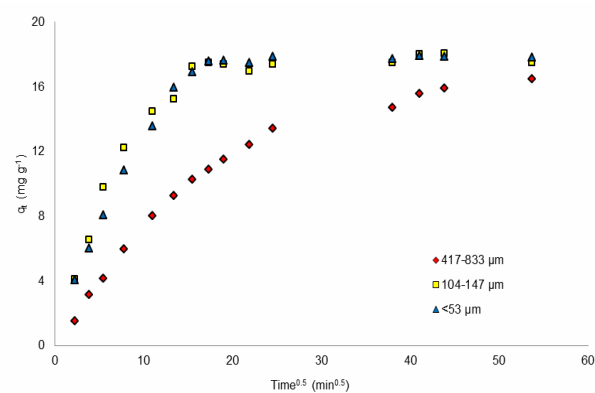
(a) Laboratory solution
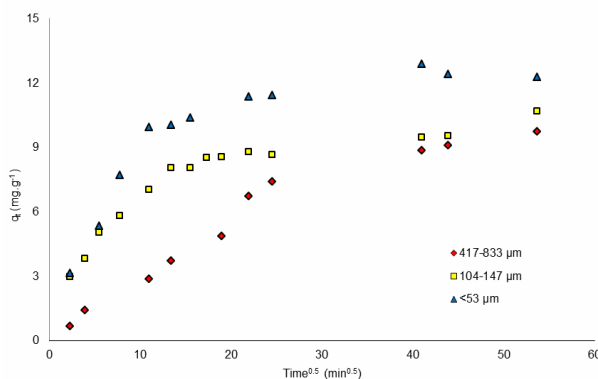
(b) AMD effluent

Figure 7: Intraparticle mass transfer for manganese removal with bone char (25 °C, 150 rpm, 2/400 g mL^{-1}): (a) Laboratory solution (C$_0$ = 100 mg L^{-1}, pH$_i$ = 5.76) and (b) AMD effluent (pH$_i$ = 5.64).

CONCLUSIONS

In this study, batch equilibrium and kinetic tests were carried out to evaluate the feasibility of using bone char for the removal of manganese from AMD effluents. Experiments using a laboratory solution containing manganese at typical concentrations were carried out for comparative analysis. The following main conclusions can be drawn based on the results obtained:

▪ Equilibrium data were adequately described by the Langmuir model and the maximum value of q$_m$ for manganese adsorption was 22 mg g^{-1} for the AMD effluent and 20 mg g^{-1} for the laboratory solution;

▪ Kinetic tests revealed that manganese removal by bone char is relatively slow (equilibrium is reached after at least 600 minutes). It could be verified that manganese loading follows a pseudo-second order model;

▪ The effect of competing species present in the AMD effluent for the bone char is significant; therefore, the pH of the effluent must be previously raised to a near neutral condition to precipitate the other metals before contact with bone char. For instance, at initial pH = 6.5, manganese removal of up to 70% was achieved, while at initial pH = 5.0 the removal was lower than 50%;

▪ The final concentration of fluoride and other metals present in the AMD effluent was in agreement with the concentration limits set forth by Brazilian law (CONAMA, 2005);

▪ Manganese removal with bone char may well involve some form of an exchange process between manganese and calcium ions;

▪ The diffusion inside particles was identified as the main rate-limiting step for manganese removal. However, when particles of smaller sizes are used, external mass transfer and intraparticle diffusion contributions may affect manganese removal.

Compared to the current treatment of AMD effluents by means of precipitation with lime, a smaller volume of sludge is expected. According to Carvalho *et al.* (2009), the removal of manganese at a pH close to neutrality reduces the volume of precipitate generated in the treatment of the effluent by 50%. In addition, the buffer effect of the bone char may prevent the need for pH correction of the effluent after treatment. Therefore, the removal of manganese from AMD effluents using bone char as an adsorbent proved to be technically feasible. More efficient removal rates of manganese are expected with the use of bone char in continuous column operations.

REFERENCES

Annadurai, G., Ling, L. Y., Lee, J. F., Adsorption of reactive dye from solution by chitosan: isotherm, kinetic and thermodynamic analysis. Journal of Hazardous Materials, 152, 337-346 (2008).

Bamforth, S. M., Manning, D. A. C., Singleton, I., Younger, P. L., Johnson, K. L., Manganese removal from mine waters - investigating the occurrence and importance of manganese carbonates. Applied Geochemistry, 21, 1274-1287 (2006).

Bosco, S. M. D., Jimenez, R. S., Carvalho, W. A., Removal of toxic metals from wastewater by Brazilian natural scolecite. Journal of Colloid and Interface Science, 281, 424-431 (2005).

Carvalho, G. X, Aguiar, A. O., Ladeira, A. C. Q., Estudo da remoção de manganês de efluentes líquidos por precipitação. In: Proc. of the XXIII Encontro Nacional de Tratamento de Minérios e Metalurgia Extrativa, Gramado, Brazil (2009). (In Portuguese).

Chen, Y.-N., Chai, L.-Y., Shu, Y.-D., Study of arsenic(V) adsorption on bone char from aqueous solution. Journal of Hazardous Materials, 160, 168-172 (2008).

Cheung, C. W., Porter, J. F., McKay, G., Sorption kinetics for the removal of copper and zinc from effluents using bone char. Separation and Purification Technology, 19, 55-64 (2000).

Choy, K. K. H., Ko, D. C. K., Cheung, C. W., Porter, J. F., McKay, G., Film and intraparticle mass transfer during the adsorption of metal ions onto bone char. Journal of Colloid and Interface Science, 271, 284-295 (2004).

CONAMA Resolution nº 357, Classificação dos corpos de água e diretrizes ambientais para o seu enquadramento, Brasília, Brazil (2005). Available on: http://www.mma.gov.br/port/conama/index.cfm (In Portuguese). (Accessed: January 15, 2012).

Ladeira, A. C. Q., Gonçalves, C. R., Uranium recovery and manganese removal from acid mine drainage. WIT Transactions on Ecology and the Environment, 111, 465-474 (2008).

Hassan, S. S. M., Awwad, N. S., Aboterika, A. H. A., Removal of mercury(II) from wastewater using camel bone charcoal. Journal of Hazardous Materials, 154, 992-997 (2008).

Ho, Y. S., Review of second-order models for adsorption systems. Journal of Hazardous Materials, B136, 681-689 (2006).

Korn, M. G. A., Santos Jr., A. F., Jaeger, H. V., Silva, N. M. S., Costa, A. C. S., Cooper, zinc and manganese determination in saline samples employing FAAS after separation and preconcentration on Amberlite XAD-7 and Dowex 1X-8 loaded with alizarin red. Journal of Brazilian Chemical Society, 15(2), 212-218 (2004).

Nascimento, M. R. L., Remoção e recuperação de urânio de águas ácidas de mina por resina de troca iônica. M.Sci. Thesis, UFSCar, São Carlos, Brazil (1998). (In Portuguese).

O'Connor, J. M., Weatherley, L. R., An investigation into the mechanism of adsorption of humic substances and trace metal compounds from potable water supplies. Global Environmental Biotechnology, 66, 91-106 (1997).

Ozawa, M., Satake, K., Suzuki, S., Removal of aqueous manganese using fish bone hydroxyapatite. Journal of Materials Science Letters, 22, 1363-1364 (2003).

Pan, X., Wang, J., Zhang, D., Sorption of cobalt to bone char: kinetics, competitive sorption and mechanism. Desalination, 249, 609-614 (2009).

Ribeiro, M. V., Uso de carvão de osso bovino na defluoretação de água para uso em abastecimento público. Belo Horizonte, M.Sci. Thesis, UFMG, Belo Horizonte, Brazil (2011). (In Portuguese).

Robinson-Lora, M. A., Brennan, R. A., Biosorption of manganese onto chitin and associated proteins during the treatment of mine impacted water. Chemical Engineering Journal, 162, 565-572 (2010).

Rocha, S. D. F., Ribeiro, M. V., Viana, P. R. M., Mansur, M. B., Bone Char: An Alternative for Removal of Diverse Organic and Inorganic Compounds from Industrial Wastewater. In: Bhatnagar, A., (Org.), Application of Adsorbents for Water Pollution, Bentham Science Publishers Ltd., Ch. 14, 502-522 (2012).

Rouquerol, J., Avnir, D., Fairbridge, C. W., Everett, D. H., Haynes, J. M., Pernicone, N., Ramsay, J. D. F., Sing, K. S. W., Unger, K. K., Recommendations for the characterization of porous sol-

ids. Pure & Applied Chemistry, 66(8), 1739-1758 (1994).

Smiciklas, I. D., Milonjic, S. K., Pfendt, P., Raicevic, S., The point of zero charge and sorption of cadmium (II) and strontium (II) ions on synthetic hydroxyapatite. Separation and Purification Technology, 18, 185-194 (2000).

Soto, O. A. J., Torem, M. L., Trindade, R. B. E., Pa-

lygorskite as a sorbent in the removal of manganese(II) from water mine effluents. In: Proc. of the XIII International Conference on Heavy Metals in the Environment, Rio de Janeiro, Brazil (2005).

Weber, W. J., Morris, J. C., Kinetic of adsorption carbon solution. Journal Sanitary Engineering Divisor, American Society Civil Engineers, 89, 31-59 (1963).